

## Relation between structural instabilities in $\text{EuTiO}_3$ and $\text{SrTiO}_3$

A. Bussmann-Holder, J. Köhler, R. K. Kremer,<sup>\*</sup> and J. M. Law

Max-Planck-Institute for Solid State Research, Heisenbergstr. 1, D-70569 Stuttgart, Germany

(Received 4 May 2011; published 24 June 2011)

Specific heat measurements and theoretical calculations reveal an intimate analogy between  $\text{EuTiO}_3$  and  $\text{SrTiO}_3$ . For  $\text{EuTiO}_3$ , a hitherto unknown specific heat anomaly is discovered at temperatures  $T_A = 282(1)\text{K}$ , which is analogous to the well-known specific heat anomaly of  $\text{SrTiO}_3$  at the temperature  $T_A = 105\text{K}$  caused by an antiferrodistortive transition. Because the zone center soft phonon mode observed in both systems can be modeled with the same parameters, we ascribe the new  $282(1)\text{K}$  instability of  $\text{EuTiO}_3$  to an antiferrodistortive phase transition. The higher transition temperature of  $\text{EuTiO}_3$  as compared to  $\text{SrTiO}_3$  results from spin-phonon coupling.

DOI: [10.1103/PhysRevB.83.212102](https://doi.org/10.1103/PhysRevB.83.212102)

PACS number(s): 63.20.-e, 75.80.+q

$\text{ATiO}_3$  ( $A = \text{Ba, Pb, Zr, Sr, Ca, Cd, or Eu}$ ) perovskites are well known for their tendencies toward numerous instabilities. Although the Ba, Pb, and Cd titanate compounds undergo ferroelectric phase transitions, the corresponding perovskite  $\text{PbZrO}_3$  exhibits an antiferroelectric phase transition.  $\text{CaTiO}_3$  (CTO),<sup>1</sup>  $\text{SrTiO}_3$  (STO),<sup>2-4</sup> and  $\text{EuTiO}_3$  (ETO)<sup>5,6</sup> show pronounced long-wave-length optic mode softening over a large temperature range but never become ferroelectric because quantum fluctuations suppress a long-range instability.<sup>7</sup> STO and CTO instead undergo an antiferrodistortive zone boundary-related structural phase transition to a tetragonal phase at temperatures  $T_A = 105\text{K}$ ,<sup>8,9</sup> and  $837\text{K}$ ,<sup>10,11</sup> respectively, which is accompanied by an extremely small lattice distortion in STO where the cubic ( $c/a$ ) lattice constant ratio changes by  $<1\%$  and a more pronounced amount in CTO.<sup>10</sup> Because of the small change of  $c/a$  in STO, it was difficult to reveal this phase transition; only from electron spin resonance (ESR),<sup>12</sup> electron paramagnetic resonance (EPR),<sup>8,13</sup> and inelastic neutron scattering (INS) data<sup>14-16</sup> could it be clearly detected. ETO, on the other hand, becomes antiferromagnetic (AFM) at temperature  $T_N = 5.5\text{K}$ ,<sup>17</sup> thereby influencing strongly the soft optic mode that abruptly increases in energy at  $T_N$ .<sup>5,6,18</sup> This latter effect has been speculated to originate from multiferroic behavior, which has substantially increased the interest in this compound. However, because a true ferroelectric instability is inhibited by quantum fluctuations, the term *multiferroic* is misleading.

Although the dynamic properties of STO are well understood, namely, originating from Ti d-band O p-band charge transfer,<sup>19</sup> those of ETO are still under discussion. In STO, both the soft zone boundary and the soft zone center mode have been shown to be caused by the configurational instability of the  $\text{O}^{2-}$  ion,<sup>20</sup> which is unstable as a free entity.<sup>21</sup> In a crystal, partial stabilization of the  $\text{O}^{2-}$  ion is achieved through interaction with the surrounding ions, but the basic tendency toward delocalization of the  $2p^6$  electrons remains. This behavior has been termed *dynamical covalency* and modeled within the polarizability model,<sup>19,22-24</sup> which is based on a double-well potential in the local core-shell coupling constant at the oxygen ion site. Because ETO has a variety of properties in common with STO—namely, optic mode softening, suppression of a ferroelectric instability by quantum fluctuations, induced ferroelectricity in strained films,<sup>25-27</sup>

identical lattice constants, and identical ionic radii of Sr and Eu—it is suggestive that the dynamics can be modeled within the same theoretical approach that has already been proven successful for STO. To model the AFM state at low temperatures, the polarizability model is extended by a spin-spin and a spin-phonon interaction term that closely resembles the one studied by Jacobsen and Stevens<sup>28</sup> except for the use of the polarizability coordinate. The Hamiltonian is given by

$$H = \sum_{i=1,2} \sum_n \left\{ \frac{p_{i,n}^2}{m_i} + \frac{f'}{2} (u_{1,n+1} - u_{1,n-1})^2 + \frac{1}{2} g_T w^2 + \frac{f}{2} [(u_{2,n} - u_{1,n} - w_{1,n})^2 + (u_{2,n-1} - u_{1,n} - w_{1,n})^2] \right\} + \sum_n \{ \hbar \varepsilon (u_{2,n+1} - u_{2,n}) S_x^{(2,n+1)} S_x^{(2,n)} + g\beta H S_z^{(2,n)} \} \quad (1)$$

with  $\beta = eh/2mc$  and  $g_T = g_2 + 3g_4 < w^2 >_T$ , where  $g_2$  is attractive. In contrast,  $g_4$  is the fourth-order repulsive anharmonic coupling term in the polarizability coordinate  $w$  that is treated in a cumulant expansion using the self-consistent phonon approximation (SPA).  $u_{i,n}$  and  $m_i$  ( $i = 1$  or  $2$ ) are displacement coordinates and masses of ions  $i$ , respectively, where  $m_1$  refers to the polarizable cluster mass  $\text{TiO}_3$  and  $m_2$  is the rigid ion mass of Eu.  $f$  and  $f'$  are nearest and second-nearest neighbor harmonic coupling constants, respectively. These coupling constants are the *same* as those derived for STO, and only the  $A$  site sublattice mass is changed to conform to the higher Eu mass. The coupling between the Eu spins  $S_x$  and  $S_z$  and the lattice,  $\varepsilon$ , is bilinear with respect to the  $A$  sublattice while the coupling between the polarization and the spin includes a third-order coupling term according to  $S_x = \omega_0 \varepsilon < S_z > / (\omega_0^2 - \omega^2) (\omega \{ 1 + g_T/2f \} + u) / \cos qa$ , which introduces higher-order couplings because  $g_T$  is analogous to Ref. 29.  $\varepsilon$  modifies the  $xy$  components of the  $g$  tensors through the lattice oscillations and varies linearly with the magnetic field  $H$ .  $S_x^{(n)}$  and  $S_z^{(n)}$  are the  $x$  and  $z$  components, respectively, of the spin at site  $n$  of the Eu atom. By introducing the definitions

$$\frac{fg_T}{2f + g_T} = \tilde{f}, \quad \frac{4f'}{m_1} \sin^2 qa + \frac{2\tilde{f}}{m_1} = \omega_1^2,$$

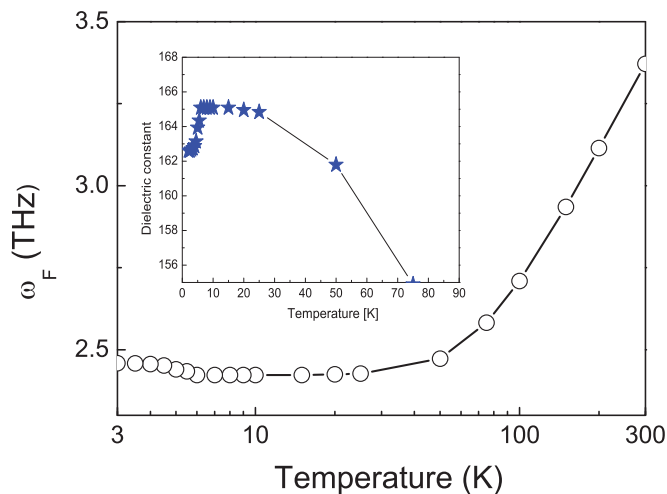


FIG. 1. (Color online) Temperature dependence of the soft optic mode  $\omega_F$  of ETO in a semilogarithmic plot. The full stars are experimental data from Refs. 5 and 6. The inset shows the related dielectric constant. Solid lines are guides to the eye.

$$\frac{4\tilde{f}\tilde{f}}{g_T m_2} \sin^2 qa + \frac{2\tilde{f}}{m_2} = \omega_2^2, \quad \omega_0^2 = \frac{g\beta H}{\hbar},$$

the corresponding dispersion relations are given by

$$\begin{aligned} (\omega^2 - \omega_1^2)(\omega^2 - \omega_2^2)(\omega^2 - \omega_0^2) - \omega_0^2 \varepsilon^2 \langle S_z \rangle (\omega^2 - \omega_1^2) \\ - \frac{4\tilde{f}^2}{m_1 m_2} \cos^2 qa (\omega^2 - \omega_0^2) = 0. \end{aligned} \quad (2)$$

The temperature dependence of  $g_T$ , where  $g_2$  and  $g_4$  are determined self-consistently within the SPA, defines the soft mode temperature dependence. For small spin-lattice coupling, the zero momentum optic mode softens with decreasing temperature, as shown in Fig. 1. In the figure, the calculated soft mode frequency is compared to the experimental data of Refs. 5 and 6, evidencing excellent agreement with the experiment. In this limit, the coupled (2) can approximately be decoupled in the long-wave-length limit to  $\omega_F^2(q=0) \approx 2\tilde{f}/\mu$ , with  $\mu$  being the reduced cell mass and  $\omega^2 = \omega_0^2$ . The soft mode has the same temperature dependence as in the uncoupled case that applies to STO. The saturation regime of  $\omega_F^2$  at temperatures  $T < 30$  K is a consequence of quantum fluctuations analogous to STO.

This regime changes if the spin-lattice coupling strength  $\varepsilon \approx H$  is switched on and long-range AFM order sets in below  $T_N$ . Again, an approximate analytic solution to (2) for the soft mode exists in this limit; for large coupling strength, i.e., large fields, the solution is given by  $\omega_F^2 = \tilde{f}/\mu + \omega_0^2 + \omega_0 \varepsilon \sqrt{|\langle S_z \rangle|}$ . In accordance with experimental data,<sup>5,6</sup> the spin-phonon coupling depresses the dielectric constant (Fig. 1, inset) and causes an anomaly at  $T_N$ , as seen experimentally. Also, at high temperatures mode-mode coupling has already set in, which induces a lowering of the zone boundary acoustic mode energy.<sup>29</sup>

The dynamical properties of ETO are well modeled by the *same* parameters as used for STO. This agreement indicates that a zone boundary-related phase transition, as realized in STO at  $T_A = 105$  K, should be present in ETO. For STO, it was recently shown that this instability arises from the same

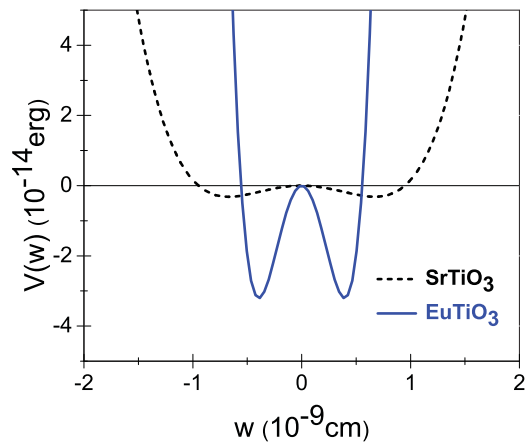


FIG. 2. (Color online) The local double-well potential of STO (black line) and of ETO (blue line). The model parameters of ETO are the same as those of STO (Ref. 28), with a mass enhancement factor of 1.73 applied to  $m_2$  to account for the heavier Eu sublattice and new self-consistently derived double-well defining parameters, namely,  $g_2 = -41.3806$  and  $g_4 = 133.5556$ .

polarizability effects as the zone center soft mode,<sup>20</sup> with the transition temperature  $T_A$  being given by

$$k_B T_A = 1/3 g_4 \left[ -g_2 + \frac{4f'f}{2f' + f} \right] \sum_{q,j=0-2} \frac{w^2(q)}{\omega_j^2(q)}, \quad (3)$$

where  $w^2$  is the polarizability coordinate eigenvector and  $\omega_j$  is defined by (2). Therefore, an analogous calculation is carried through for ETO with the distinction that the second-nearest neighbor interaction is more attractive than in STO because of the spin-phonon coupling term. From this calculation, an antiferrodistortive phase transition is predicted to occur at  $T \approx 298$  K. Similar strong spin-phonon coupling has been observed in the rare earth manganites,<sup>30-33</sup> where even a hybridized soft mode magnon excitation has been detected by INS.<sup>34</sup>

The self-consistently derived double-well potentials differ distinctively between STO and ETO (Fig. 2). Although in STO the potential is broad with a shallow minimum, it is narrow and deep in ETO. This finding implies that the STO dynamics are more on the displacive side whereas in ETO order/disorder type dynamics are realized, which has already been addressed in Refs. 35-37. By producing mixed STO-ETO crystals, an interesting crossover between both should occur.

To test the preceding prediction, ETO samples were prepared by carefully mixing dried  $\text{Eu}_2\text{O}_3$  (Alfa, 99.99%) with  $\text{Ti}_2\text{O}_3$  powder (Alfa, 99.99%), in a 1:1 ratio in an agate mortar under Ar. Then the powder was pressed to a pellet and heated in a corundum tube under Ar for 4 d at 1400 °C. The ETO sample was dark gray with a cubic lattice constant of 390.6(1) pm at room temperature, according to x-ray powder diffraction data. A further temperature-dependent x-ray diffraction scan did not reveal any deviations from cubic symmetry, thus seemingly disproving the expected existence of a phase transition. However, a similar experience occurred with STO, where initially only ESR, EPR, and INS<sup>8,12-16</sup> were able to see the phase transition. Later, specific heat measurements also detected a tiny anomaly at  $T_A$  in STO.<sup>38-41</sup> Therefore, specific heat measurements (relaxation-type calorimeter physical properties

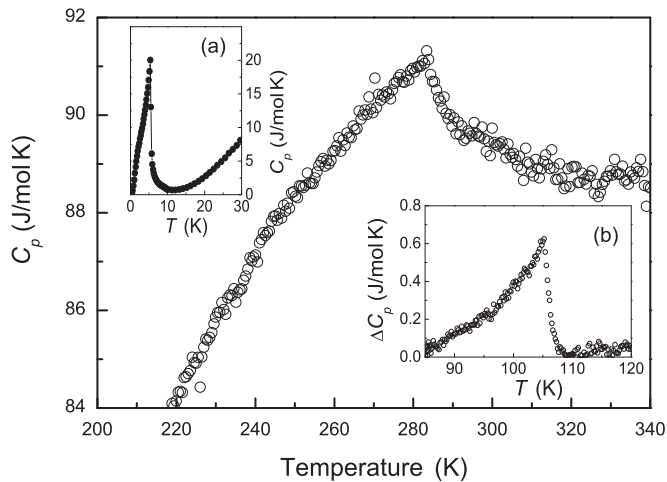


FIG. 3. Specific heat of ETO as a function of temperature in the temperature range around the phase transition. The insets show (a) the low temperature region around  $T_N$  with the  $\lambda$ -type anomaly in the specific heat and (b) the specific heat anomaly  $\Delta C_p$  of STO around the 105K transition. A background similar to the procedure suggested by Salje *et al.* (Ref. 44) was subtracted.

measurement system, Quantum Design) were first repeated for STO (commercially available samples) and then carried through for ETO (Fig. 3). In STO, the structural instability causes an obvious anomaly in the specific heat at 105K (Fig. 3 inset (b)), which is seen much more clearly in the present experiment than in the previous ones.<sup>38–41</sup> In ETO, an anomaly similar in shape and magnitude to that of STO is seen at 282(1) K, close to the theoretically expected phase transition temperature. In addition, the transition to the AFM state is evident in the specific heat data as a  $\lambda$ -type anomaly (Fig. 3 inset (a)).

To exclude the phase transition at 282(1) K from being related to some magnetic ordering stemming from the Eu spins, the magnetic susceptibility was carefully measured and found to be in best agreement with existing data.<sup>17,42,43</sup> Although at  $T_N = 5.5$  K a deviation from linearity is clearly seen corresponding to the AFM transition temperature, deviations from the Curie law occurring at  $T_A = 282(1)$  K could not be detected. Therefore, we concluded that the specific heat anomaly at this temperature stems from a structural phase transition. The analogies between STO and ETO suggest that this is of antiferrodistortive origin with extremely small changes in the cubic axis relation, which obscures its detection by infrared or Raman scattering techniques. To further substantiate this conclusion, we propose performing INS experiments on ETO, where the modeling predicts an acoustic mode boundary softening. An additional support is also expected to come from ESR, EPR, and Mössbauer measurements, where a line splitting or broadening should appear at 282(1) K.

In summary, a phase transition is predicted to exist in ETO, analogous to that in STO, wherein the oxygen octahedral tilt is at the theoretical transition temperature  $T_A \approx 298$  K. The prediction was confirmed experimentally by specific heat measurements, which in comparison to STO clearly demonstrate its existence—however, at  $T_A = 282(1)$  K. In addition, the AFM transition is detected as a  $\lambda$ -type anomaly at  $T = 5.5$  K. Although theory and experiment both reveal close analogies between STO and ETO, a distinctive difference in the dynamics exists, namely, that ETO is more on the order/disorder side whereas STO is in the displacive limit.

A.B.H. acknowledges many useful discussions with S. Kamba.

\*rekre@fkf.mpg.de.

<sup>1</sup>V. V. Lemanov, A. V. Sotnikov, E. P. Smirnova, M. Weihnacht, and R. Kunze, *Solid State Commun.* **110**, 611 (1999).

<sup>2</sup>H. Burkhard and K. A. Müller, *Helv. Phys. Acta* **49**, 725 (1976).

<sup>3</sup>H. Uwe and T. Sakudo, *Phys. Rev. B* **13**, 271 (1976).

<sup>4</sup>W. Cochran, *Adv. Phys.* **9**, 387 (1960).

<sup>5</sup>S. Kamba, D. Nuzhnyy, P. Vaněk, M. Savinov, K. Knížek, Z. Shen, E. Šantavá, K. Maca, M. Sadowski, and J. Petzelt, *Europhys. Lett.* **80**, 27002 (2007).

<sup>6</sup>V. Goian, S. Kamba, J. Hlinka, P. Vaněk, A. A. Belik, T. Kolodiaznyy, and J. Petzelt, *Eur. Phys. J. B* **71**, 429 (2009).

<sup>7</sup>K. A. Müller and H. Burkhard, *Phys. Rev. B* **19**, 3593 (1979).

<sup>8</sup>K. A. Müller, *Phys. Rev. Lett.* **2**, 341 (1959).

<sup>9</sup>P. A. Fleury, J. F. Scott, and J. M. Worlock, *Phys. Rev. Lett.* **21**, 16 (1968).

<sup>10</sup>L. C. Walters and R. E. Grace, *J. Phys. Chem. Solids* **28**, 824 (1967).

<sup>11</sup>J. S. Kim, M. Itoh, and T. Nakamura, *J. Solid State Chem.* **101**, 77 (1992).

<sup>12</sup>H. Unoki and T. Sakudo, *J. Phys. Soc. Jpn.* **23**, 546 (1967).

<sup>13</sup>E. J. Kirkpatrick, K. A. Müller, and R. S. Rubins, *Phys. Rev. A* **135**, 86 (1964).

<sup>14</sup>G. Shirane and Y. Yamada, *Phys. Rev.* **177**, 858 (1969).

<sup>15</sup>R. A. Cowley, W. J. L. Buyers, and G. Dolling, *Solid State Commun.* **7**, 181 (1969).

<sup>16</sup>J. M. Worlock, J. F. Scott, and P. A. Fleury, in *Light Scattering Analysis of Solids*, edited by G. B. Wright (Springer, New York, 1969), p. 689.

<sup>17</sup>T. R. McGuire, M. W. Shafer, R. J. Joenk, H. A. Halperin, and S. J. Pickart, *J. Appl. Phys.* **37**, 981 (1966).

<sup>18</sup>T. Katsufuji and H. Takagi, *Phys. Rev. B* **64**, 054415 (2001).

<sup>19</sup>A. Bussmann-Holder and H. Büttner, *Nature (London)* **360**, 541 (1992).

<sup>20</sup>A. Bussmann-Holder, H. Büttner, and A. R. Bishop, *Phys. Rev. Lett.* **99**, 167003 (2007).

<sup>21</sup>A. Bussmann-Holder, H. Bilz, R. Roenspiess, and K. Schwarz, *Ferroelectrics* **25**, 343 (1980).

<sup>22</sup>R. Migoni, H. Bilz, and D. Bäuerle, *Phys. Rev. Lett.* **37**, 1155 (1976).

<sup>23</sup>H. Bilz, A. Bussmann, G. Benedek, H. Büttner, and D. Strauch, *Ferroelectrics* **25**, 339 (1980).

<sup>24</sup>H. Bilz, H. Bilz, G. Benedek, and A. Bussmann-Holder, *Phys. Rev. B* **35**, 4840 (1987).

<sup>25</sup>J. H. Lee *et al.*, *Nature* **466**, 954 (2010).

- <sup>26</sup>N. A. Partsev, A. K. Tagantsev, and N. Setter, *Phys. Rev. B* **61**, R825 (2000).
- <sup>27</sup>J. H. Haeni *et al.*, *Nature* **430**, 758 (2004).
- <sup>28</sup>E. H. Jacobsen and K. W. H. Stevens, *Phys. Rev.* **129**, 2036 (1963).
- <sup>29</sup>V. V. Shvartsman, P. Borisov, W. Kleemann, S. Kamba, and T. Katsufuji, *Phys. Rev. B* **81**, 064426 (2010).
- <sup>30</sup>S. Petit, F. Moussa, M. Hennion, S. Pialhès, L. Pinsard-Gaudart, and A. Ivanov, *Phys. Rev. Lett.* **99**, 266604 (2007).
- <sup>31</sup>H. J. Lewtas, A. T. Boothroyd, M. Rotter, D. Prabhakaran, H. Müller, M. D. Lee, B. Roessli, J. Gavilano, and P. Bourges, *Phys. Rev. B* **82**, 184420 (2010).
- <sup>32</sup>X. Fabrèges, S. Petit, I. Mirebeau, S. Pialhès, L. Pinsard, A. Forget, M. T. Fernandez-Diaz, and F. Porcher, *Phys. Rev. Lett.* **103**, 067204 (2009).
- <sup>33</sup>T. Chatterji, *Pramana J. Phys.* **71**, 847 (2008).
- <sup>34</sup>D. Senff, P. Link, K. Hradil, A. Hiess, L. P. Regnault, Y. Sidis, N. Aliouane, D. N. Argyriou, and M. Braden, *Phys. Rev. Lett.* **98**, 13720 (2007).
- <sup>35</sup>H. Wu, Q. Jiang, and W. Z. Shen, *Phys. Rev. B* **69**, 014104 (2004).
- <sup>36</sup>Q. Jiang and H. Wu, *J. Appl. Phys.* **93**, 2121 (2003).
- <sup>37</sup>H. Wu, Q. Jiang, and W. Z. Shen, *Phys. Lett. A* **330**, 358 (2004).
- <sup>38</sup>P. R. Garnier, *Phys. Lett. A* **35**, 413 (1971).
- <sup>39</sup>V. Franke and E. Hegenbarth, *Phys. Status Solidi* **25**, K17 (1974).
- <sup>40</sup>I. Hatta, Y. Shiroishi, K. A. Müller, and W. Berlinger, *Phys. Rev. B* **16**, 1138 (1977).
- <sup>41</sup>M. C. Gallardo, R. Burriel, F. J. Romero, F. J. Gutiérrez, and E. K. H. Salje, *J. Phys. Condens. Matter* **14**, 1881 (2002).
- <sup>42</sup>H. Wu and W. Z. Shen, *Solid State Commun.* **133**, 487 (2004).
- <sup>43</sup>C.-L. Chien, S. DeBenedetti, and F. De S. Barros, *Phys. Rev. B* **10**, 3913 (1974).
- <sup>44</sup>E. K. H. Salje, M. C. Gallardo, J. Jiménez, F. J. Romero, and J. Del Cerro, *J. Phys. Condens. Matter* **10**, 5535 (1998).